WHITTAKER CORPORATION
Narmco Research & Development Division,
San Diego, California

RESEARCH STUDY OF COMMON BULKHEAD AND MANUFACTURING TECHNOLOGY IMPROVEMENT PROGRAM FOR SATURN STAGES

FINAL REPORT

Contract NAS8-20376

Covering Period 23 June 1966 through 23 June 1967

by

Stephen Feher

Prepared for

GEORGE C. MARSHALL SPACE FLIGHT CENTER
Huntsville, Alabama

RESEARCH STUDY OF COMMON BULKHEAD AND MANUFACTURING TECHNOLOGY IMPROVEMENT PROGRAM FOR SATURN STAGES

by

Stephen Feher

FOREWORD

This report was prepared by Whittaker Corporation, Narmco Research & Development Division, San Diego, California, under Contract NAS 8-20376, entitled "Research Study of Common Bulkhead and Manufacturing Technology Improvement Program for Saturn Stages." This program was administered by the National Aeronautics and Space Administration, George C. Marshall Space Flight Center, Huntsville, Alabama. Mr. Lawrence Garrison was the Contracting Officer. Mr. B. K. Davis performed the function of Contracting Officer's Representative. He maintained close coordination with Narmco and provided valuable technical guidance during the course of this program.

This report was released by the authors for publication on 10 July 1967.

Work was conducted at Narmco under the general direction of Mr. Boris Levenetz, Assistant Manager of the Engineering Department. Mr. Stephen Feher served as Principal Investigator, and received assistance from Mr. Roger Radcliffe, Engineer.

ABSTRACT

The purpose of this study program was to determine the shear stress distribution in the adhesive layer of bonded joints, using photoelastic stress analysis techniques, to establish the effect of joint configuration, bondline thickness, and adhesive modulus on the structural efficiency of bonded joints, Birefringent resin materials were evaluated for use as adhesives and coatings at room temperature and cryogenic temperature suitable for direct and indirect photoelastic analysis of the adhesive layer stress distributions. Experimental shear stress distribution data were obtained by the photoelastic technique on several joint configurations, using various adhesives. A theoretical stress analysis was also conducted so that results could be compared with experimental findings. Based on the results of this investigation, recommendations are made for the achievement of higher structural efficiency in bonded joint designs by optimization of configuration and proper selection of adhesives, Recommendations are also made for further experimental and analytical studies for the development of improved design and fabrication methods for bonded joints.

TABLE OF CONTENTS

LIST OF ILLUSTRATIONS

NOMENCLATURE

a,b	arbitrary constants
2c	joint length, in.
d	displacement, in.
E	modulus of elasticity of adherend, psi
e	base of natural logarith
G_c	shear modulus of the adhesive, psi
K	photoelastic sensitivity factor
M	bending moment
P	load, lb
p	stress in the adherend, psi
T	axial load in adherend, lbs
u	displacement of adherend, in.
x	distance along the joint, in.
λ	shear strain, radians
η	bondline thickness, in.
τ	shear stress, psi

Subscripts:

a	adhesive
l	lower
max	maximum
u	upper
ult	ultimate

SECTION I

INTRODUCTION

The application of adhesive-bonded joints in primary structures has gained wide acceptance in modern aerospace design practice during the past decade. However, the full potential of lighter weight and manufacturing simplicity offered by bonded structural joints has not yet been realized in actual design proactice because of the low efficiency of most bonded joints based on current design and fabrication methods.

The primary criterion for efficient joint design is the achievement of uniform stress distribution in the bonding agents, allowing the full utilization of the strength of the adhesive. Localized stress concentration and the uncertainty of the magnitude of these stresses cause the designer to apply safety factors in the sizing of bonded joints which are well in excess of common practice used for other structural components.

The problem of structural design optimization of adhesive-bonded joints has been treated by several investigators.[1-3] Due to the complexity of the problem, however, theoretical studies have produced only limited results derived through idealized models not widely applicable to actual design problems. The large number of variables involved when all important adherend and adhesive properties which affect the performance of bonded joints are taken into consideration (including geometric configurations) dictates that theoretical analysis be supplemented with experimental investigations.

The purpose of this program was to utilize photoelastic experimental stress analysis techniques for the study of shear stress distribution in bonded joints to establish the effect of configuration and adhesive properties on the efficiency of the bonded joint.

Photoelastic stress analysis techniques are well suited for this application because of their ability to provide a quantitative measure of the magnitude of stresses over a large continuous area and, at the same time, to give a pictorial presentation of the distribution and direction of these stresses.

Two basically different photoelastic stress analysis techniques were employed during this program for the measurement of shear stress distribution in the adhesive layer of bonded joints. The first technique was based on the use of adhesive materials which exhibit birefringency under variations in stresses within the adhesive layer when illuminated with circularly polarized light. This phenomenon can be put to use to determine stress distribution in the adhesive layer by using a transparent material, such as glass, on one of the adherends of the joint to provide a reflective mirror finish on the bonded surface of the other adherend. When viewed by a reflective polariscope through the glass adherend, the birefringent pattern in the adhesive layer can be analyzed while the joint specimen is being loaded mechanically. With the second technique, the need for a

transparent adherend is eliminated and a birefringent plastic material is used as a coating over the outside surface of the adherends, A reflective polariscope is also used with this technique for viewing the birefringent pattern in the plastic coating while the joint is being loaded mechanically, However, the measured stress distributions corresponding to the birefringent patterns are, in this case, the plane stresses in the adherend rather than the stresses in the adhesive layer. But the shear stress distribution in the adhesive layer can be obtained from the measured stress distribution in the adherends by direct differentiation. This second technique, commonly referred to as the photostress analysis, is advantageous in that experimental stress analysis of a real joint specimen can be made using typical structural adherend materials and adhesives. In other words, the joint models to be analyzed are not restricted to the use of birefringent adhesives or transparent adherend.

SECTION II

TECHNICAL INVESTIGATION

DIRECT MEASUREMENT OF SHEAR STRESS DISTRIBUTION

The initial objective of the program was to investigate the feasibility of the direct measurement of shear stress distribution in the adhesive layer of bonded joints. Based on the known birefringent characteristics of certain resin materials, we assumed that by using a transparent adherend on one side of the joint, the birefringent pattern produced in the adhesive layer under varying stress levels could be observed by a reflective polariscope. This approach was contingent upon the assumption that the other adherend or the back side of the adhesive layer would render a reflective mirror surface.

The successful, practical application of this technique is largely dependent on the sensitivity of the birefringent resin material. The first task of the program, therefore, was to evaluate the sensitivity of several birefringent resins.

Resin Screening Tests

The sensitivity of a birefringent resin is defined by the magnitude of fringe order produced in the material subject to a given mechanical strain level.

A single calibration fixture, shown in Figure 1, was used to evaluate several candidate resin ,systems. With this fixture, a 1/4-in. thick aluminum beam coated with a thin layer of resin is fixed on one end, while the other end is deflected a known amount. The birefringent fringe order in the plastic coating is measured at several points by a reflective polariscope. (The reflective polariscope and its use are discussed briefly in Appendix A.) The magnitude of axial strain can be calculated for the aluminum beam, thus permitting test data to be obtained on the fringe order versus strain for the resin coating,

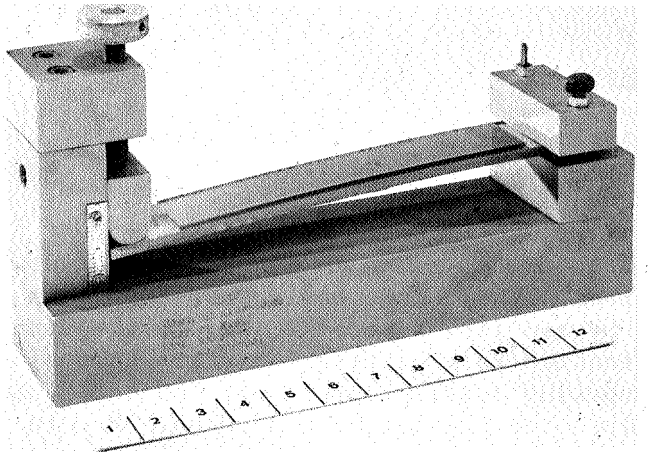

Figure 1. Photoelastic Calibration Setup

Si:: resin systems were evaluated, using the beam calibration fixture at room temperature and when submerged in liquid nitrogen. The birefringent sensitivity of these resins is presented in Table I. As indicated by the lack of data at cryogenic temperature for all but two of the candidate resins, most of the materials investigated are not suitable for use at liquid nitrogen temperatures because of their failure under thermal stresses. In the case of the very low-modulus Narmco 7343 material, the lack of data is due to the very low birefringent sensitivity of this resin, both at room temperature and at cryogenic temperature. This material can withstand the thermal schock, however, when submerged in liquid nitrogen. The special optically clear cryostat used in the photoelastic measurements of the specimens submerged in liquid nitrogen is illustrated and described in Appendix B.

TABLE I

BIREFRINGENT SENSITIVITY OF RESIN SYSTEMS

Adhesive	Sens tivity	
	RT	-320°F
Budd Company L-11	0.13	--*
Ciba 6020/HN 951	0.09	0.10
Epon 828/1031	0.09	--*
Narmco 7344	0.06	0.08
Epon 828/Versamid 125	0.04	--*
Narmco 7343	--*	--*

* No data.

Birefringent Adhesive Selection

The Ciba 6020/951 adhesive was selected for future use in the program in both room temperature and cryogenic tests. Based on the results of the adhesive screening program, the Ciba 6020/951 demonstrated high photoelastic sensitivity (i.e., a fringe order coefficient of 0.09 at room temperature and of 0.10 at -320°F), and appeared to be suitable for use at cryogenic temperature in thin layers. Other important factors leading to the selection of the Ciba adhesive were that specimen fabrication was easily accomplished because of its room temperature cure and that low residual stresses were obtained as a result of its low shrinkage characteristics.

Glass/Metal Joint Tests

Bonded joint specimens, for the direct measurement of shear stress distribution in the adhesive layer, were fabricated with the Ciba adhesive and with glass and metal adherends.

The first joint specimen, shown in Figure 2, consisted of an aluminum strip bonded to a glass plate. The bondline was 0.020 in. thick. The joint was loaded in shear by applying a tensile load to the aluminum strip while the glass plate was restrained in a holding fixture. Photoelastic measurements made during the increasing loading conditions indicated uniform stress distribution in the adhesive over the entire bond area. However, the maximum fringe order obtained was only about 0.65 when bond failure occurred at the glass/adhesive interface. Theoretical shear stress distribution calculations gave

indication that the thick bondline used in this specimen results in only very small stress risers at the ends of the bonded area. In order to observe typical bondline shear stress distribution with large stress risers, a specimen with thinner bondline will have to be fabricated.

The second specimen, illustrated graphically in Figure 3, had a 0.010-in. thick bondline. We anticipated that higher loading of this thin bondline would be required to permit photoelastic measurements. The specimen geometry was therefore modified to eliminate direct loading of the glass plates. In this configuration, two glass plates were used as doublers over two aluminum strips loaded in tension. Photoelastic measurement of the stress distribution in the adhesive was not successful because of the bond failure at the glass/adhesive interface.

With the experience gained from the unsuccessful results of these two specimen configurations, a new set of joint specimens was fabricated, using high-quality tempered Vycor glass bonded to aluminum with Ciba 6020/951 and Narmco *7344* adhesives (see Figure *4)*. These specimens failed at a very low load level. The glass plates cracked longitudinally in the doubler area, which indicates that these failures were a result of residual thermal stresses caused by mismatched thermal strains of the Vycor glass and the aluminum doublers.

This situation might have been corrected by using thinner doublers made of a metal having a lower thermal expansion than aluminum. However, the indirect measurement of adhesive shear stress distributions, initiated as a parallel course of study with the direct measurement attempts, was showing very promising results. Further efforts in direct measurements were therefore abandoned in favor of the indirect technique.

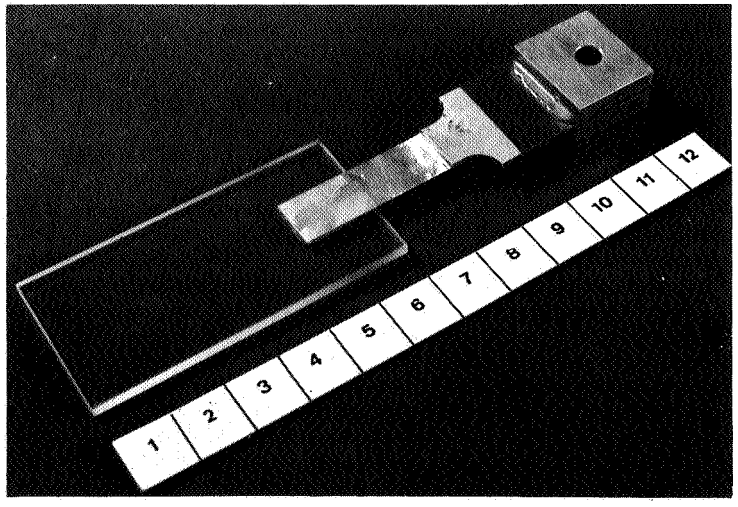

Figure 2. Glass-Metal Joint of Single Lap Configuration

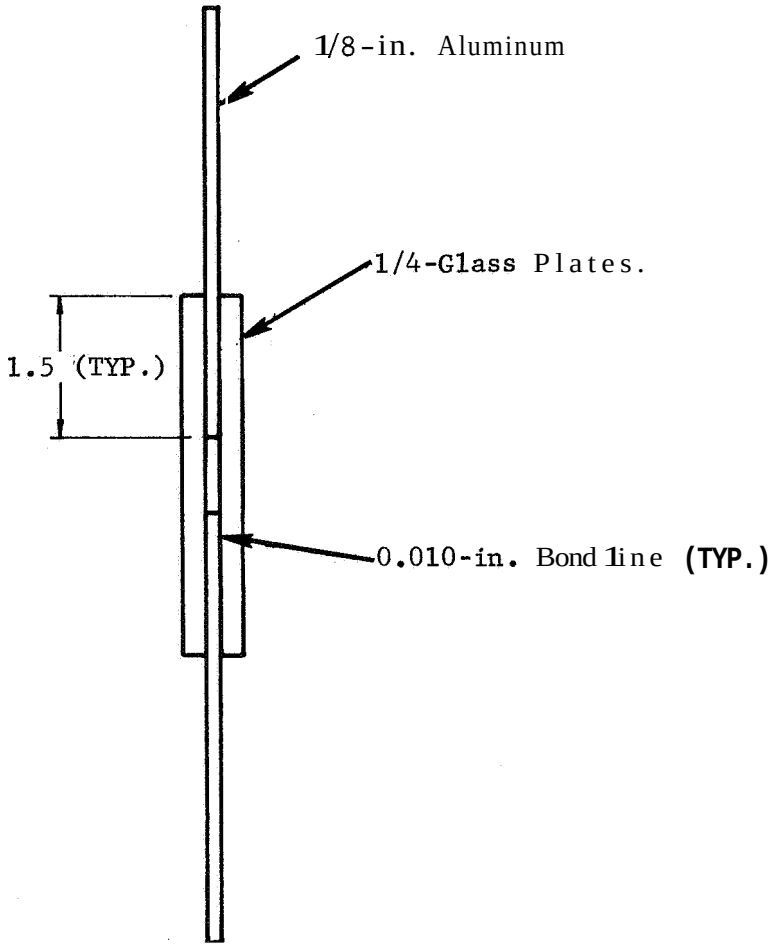

Figure 3. Glass-Metal Joint Double Lap Configuration

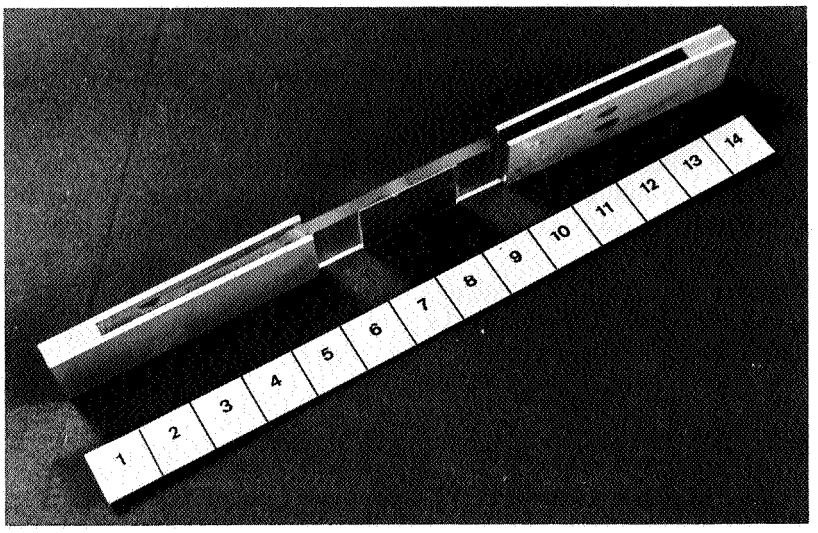

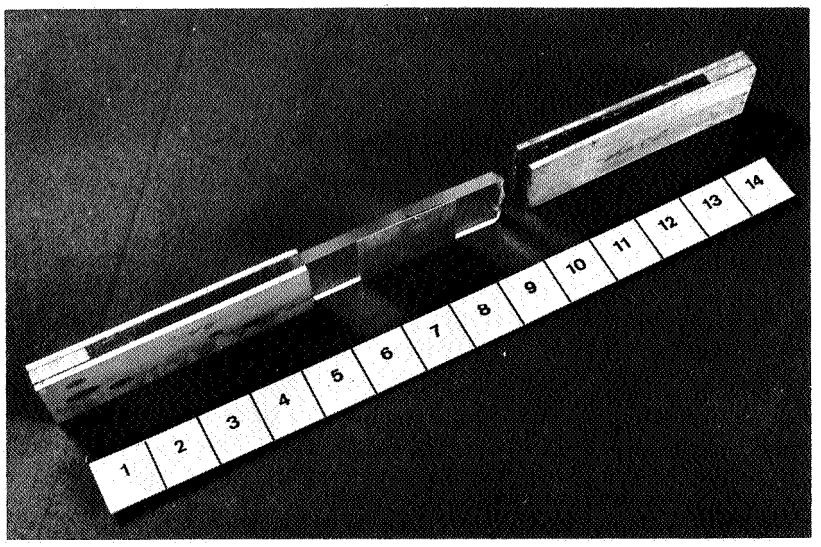

Figure 4. Vycor Glass/Metal Joints of Single Lap Configuration. Aluminum doubler

INDIRECT MEASUREMENT OF SHEAR STRESS DISTRIBUTION

Indirect measurement of the shear stress distribution in the adhesive layer of bonded joints was accomplished by application of a birefringent plastic coating over the outside surfaces of the adherends. Photoelastic analysis of the coatings provides the means to measure the stress distribution in the adherends. As long as these adherends are relatively thin, in comparison to the length of the bonded joint, the stress distribution in the adherend can be assumed to be two-dimensional with no variation in the thickness direction. In other words, the stress distribution measured on the surface of the adherend is identical to the stresses throughout the thickness of the adherend. This plane stress condition permits us to calculate the shear stress distribution in the adhesive layer by direct differentiation of the axial stress distribution obtained for the adherend.

The plane stress condition only holds true, however, in the case of lap joints with no bending. Therefore, the indirect measurement of adhesive shear stress distribution was limited to symmetrical double lap joints.

Experimental Stress Analysis of Double Lap Joints

The birefringent plastic coating, photoelastic stress analysis technique is generally known as the photostress method. The first two joint specimens analyzed by the photostress method are shown in Figures 5 and 6.

The two specimens were identical except for the doubler configuration, The first joint has plane 0.063-in. thick aluminum doublers on both sides of the 0.250-in. thick aluminum main plates, while the second specimen represents the fingered doubler pattern used on the Saturn common bulkhead.

Figures 7 and 8 show the results of the photostress analysis, and illustrate the axial stress distribution in the doublers and the shear stress distribution curves obtained by differentiation of the axial stress distribution.

In the case of the plane doubler, the shear stress distribution curve obtained by the indirect method is in good agreement with the general shape of the theoretical shear stress distribution predicted by Volkersen[4] for lap joints without bending. The only significant deviation of the experimental stress distribution from the theoretical prediction occurs at the ends of the bondline, where the theoretical distribution has its maximum points, while the experimental curves shown a sharp reduction in the measured shear stress.

The rounded-off shape of the experimental shear stress distribution curve is probably the effect of non-uniform stress distribution through the thickness of the doubler near the ends, In other words, our basic assumption of two-dimensional stress distribution in the doubler does not hold true near the ends of these relatively thick doublers. The use of thinner doubler is required for the realistic measurement of the shear stress distribution in the adhesive layer by the indirect method.

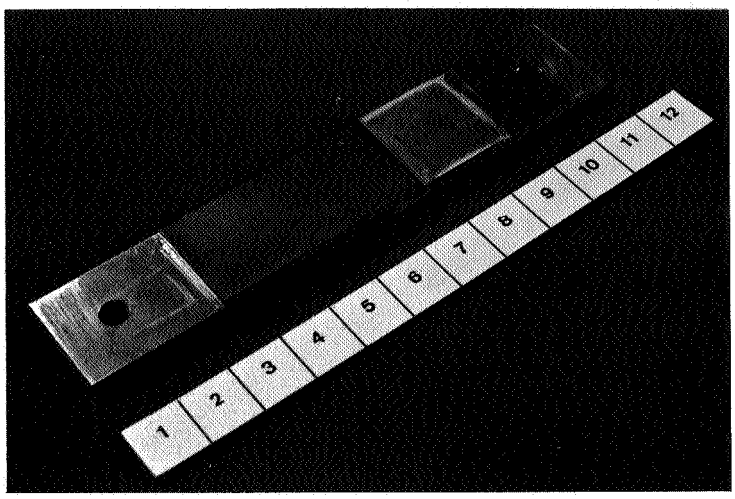

(a) Double Lap Bonded Joint with Photostress Coating

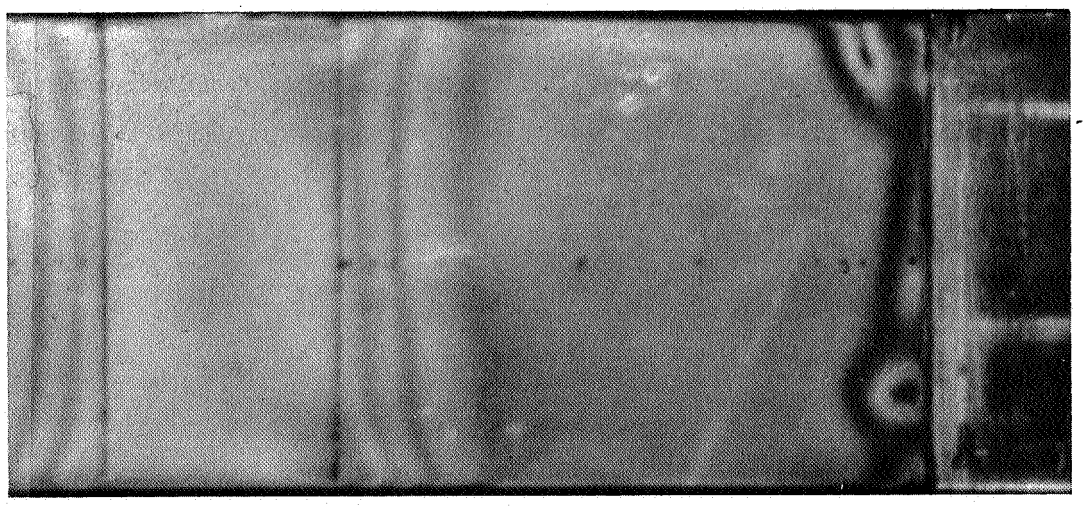

(b) Bhotoelastic Fringe Pattern at 10,000-lb Load

Figure 5. Plain Joint Specimen

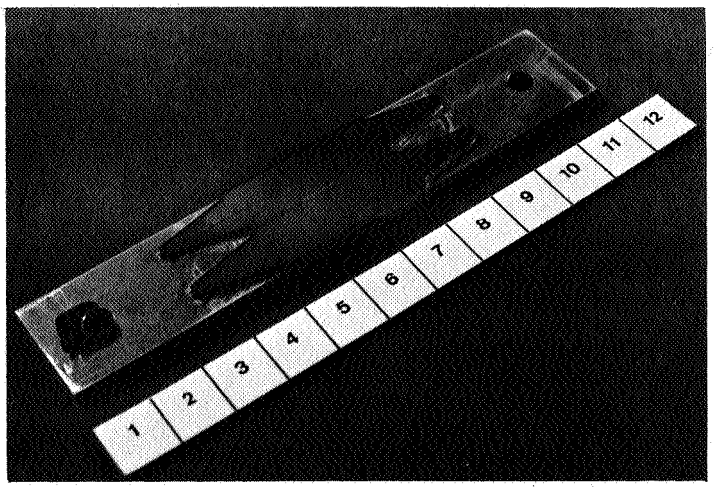

(a) Fingered Doubler Double Lap Bonded Joint with Photostress Coating

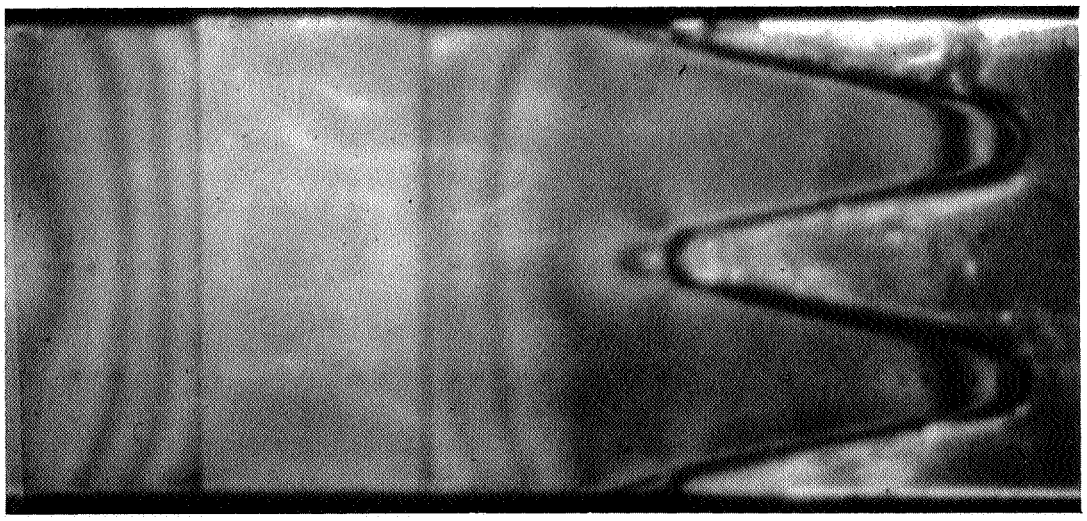

(b) Photoelastic Fringe Pattern at 10,000-lb Load

Figure 6. Fingered Doubler Joint Specimen

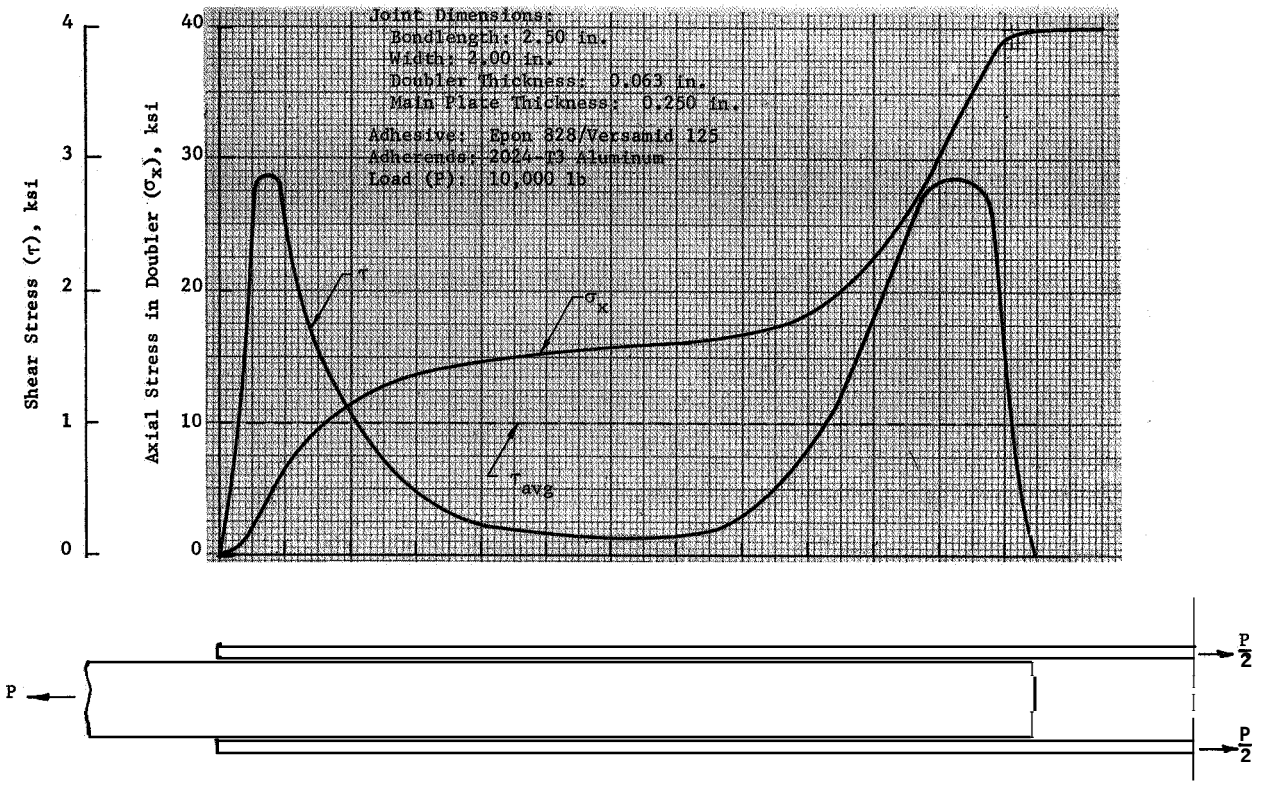

Figure 7. Stress Distribution in a Plane Doubler Double Lap Bonded Joint (Determined by photostress measurement technique)

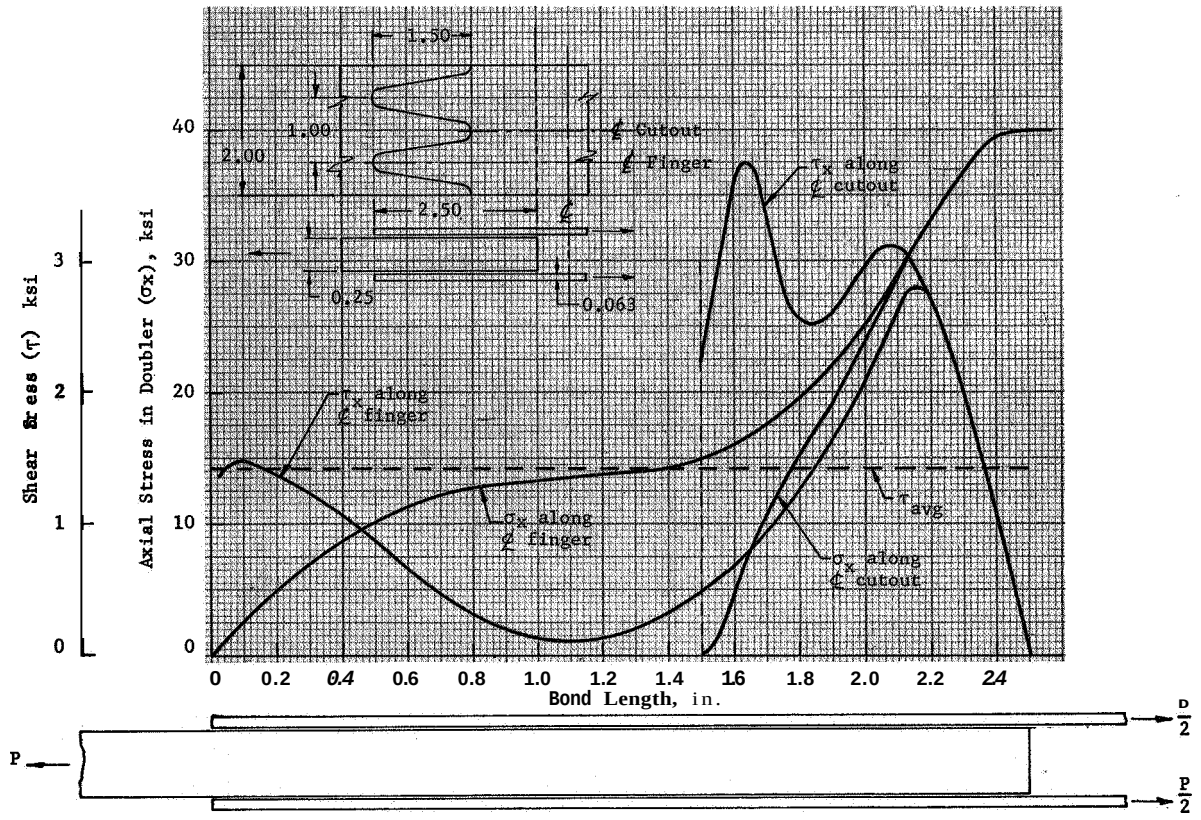

Figure 8. Stress Distribution in a Fingered Doubler Doable Lap Bonded Joint (Determined by photostress measurement technique)

The shear stress distribution curves obtained for the fingered doubler joint are much harder to evaluate in terms of agreement with theoretical prediction because of the complexity of such analyses. We can definitely conclude from the experimental shear stress distribution, however, that the fingered pattern resulted in a reduction of the maximum stress concentration at the free ends of the doubler, while causing only a small stress rise at the center of the cutout section.

Based on the successful analysis of these two initial joint specimens, six additional double lap joint models were analyzed, representing three types of configurations depicted in Figure 9. Two sets of joints with these configurations were investigated using two different adhesive systems. Photoelastic measurements of the six specimens were made at several load levels. A typical set of fringe patterns for the three types of joint configurations is shown in Figure 10.

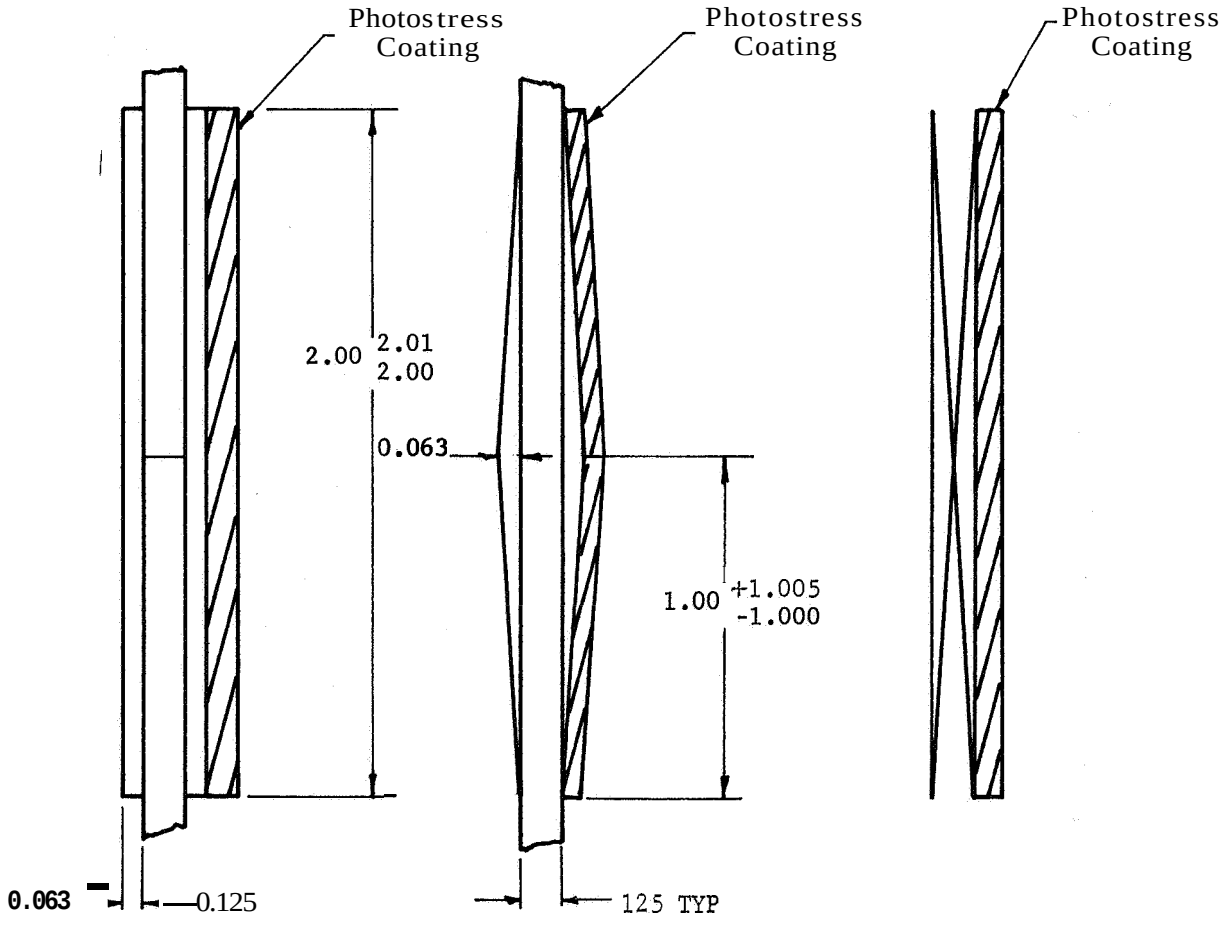

Figure 9. Bonded Double Lap Joint Configurations

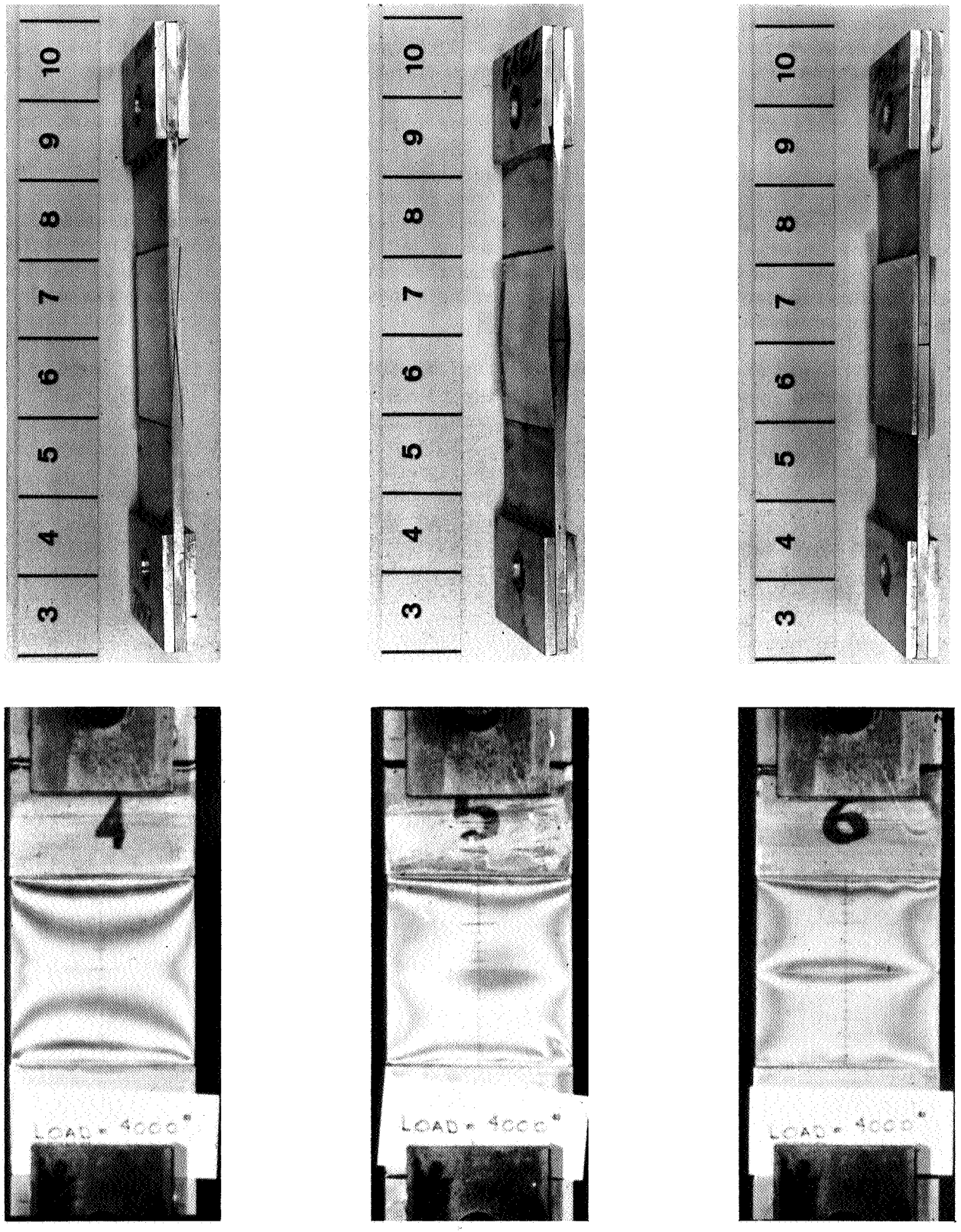

Figure 10. Double Lap Bonded Joint Specimens and Photoelastic Fringe Patterns at 4000-lb Applied Load

The stress distributions calculated for the six joint specimens from the photostress data are presented in Figures 11 through 16. The first three joints were bonded with the high-modulus Epon 828/Versamid 125 adhesive, while Specimens 4 through 6 were bonded with the low-modulus Narmco 7343 adhesive.

Theoretical shear stress distribution curves are also presented for Specimens 1 and 4 (Figures 11 and 14 respectively). These theoretical curves were calculated by using an improved version of the classical joint analysis techniques. This modified approach forms the basis for realistic treatment of the adhesive layer behavior throughout the elastic and plastic range by utilizing an experimentally obtained shear stress versus shear strain relationship. A more detailed discussion of the theoretical analysis is presented in the following section, and the mathematical formulation of the analysis is given in Appendix C.

The shear stress distributions obtained for the three different joint configurations were first compared. The plane doubler joint demonstrated the familiar shear stress distribution curve, characterized by the nearly symmetrical high stress concentrations at both ends of the bondline. There is generally good agreement between experimental and theoretical shear stress distribution for the epoxy-bonded joint except at the end points.

The discrepancy in the case of the Narmco 7343 bonded plane doubler joints is much larger. This is attributable to the large variation in the shear modulus of this adhesive, which is very sensitive to moisture absorption in the bondline. The test data used in the theoretical analysis were obtained from specimens prepared without the application of special primer and moisture absorption preventing processes, while the joint models used in the experimental stress analysis were bonded following the best available processing techniques.

Comparing the shear stress distributions of the plane doubler joints with the tapered doubler type and with the tapered doubler scarfed joint configuration indicates a definite trend of reduction in the maximum stress concentration. The tapered double-scarfed joint demonstrates a shear stress distribution approaching a uniformly stressed adhesive layer. The joints bonded with the lower modulus adhesive appear to have reduced stress concentrations in the case of all three joint configurations.

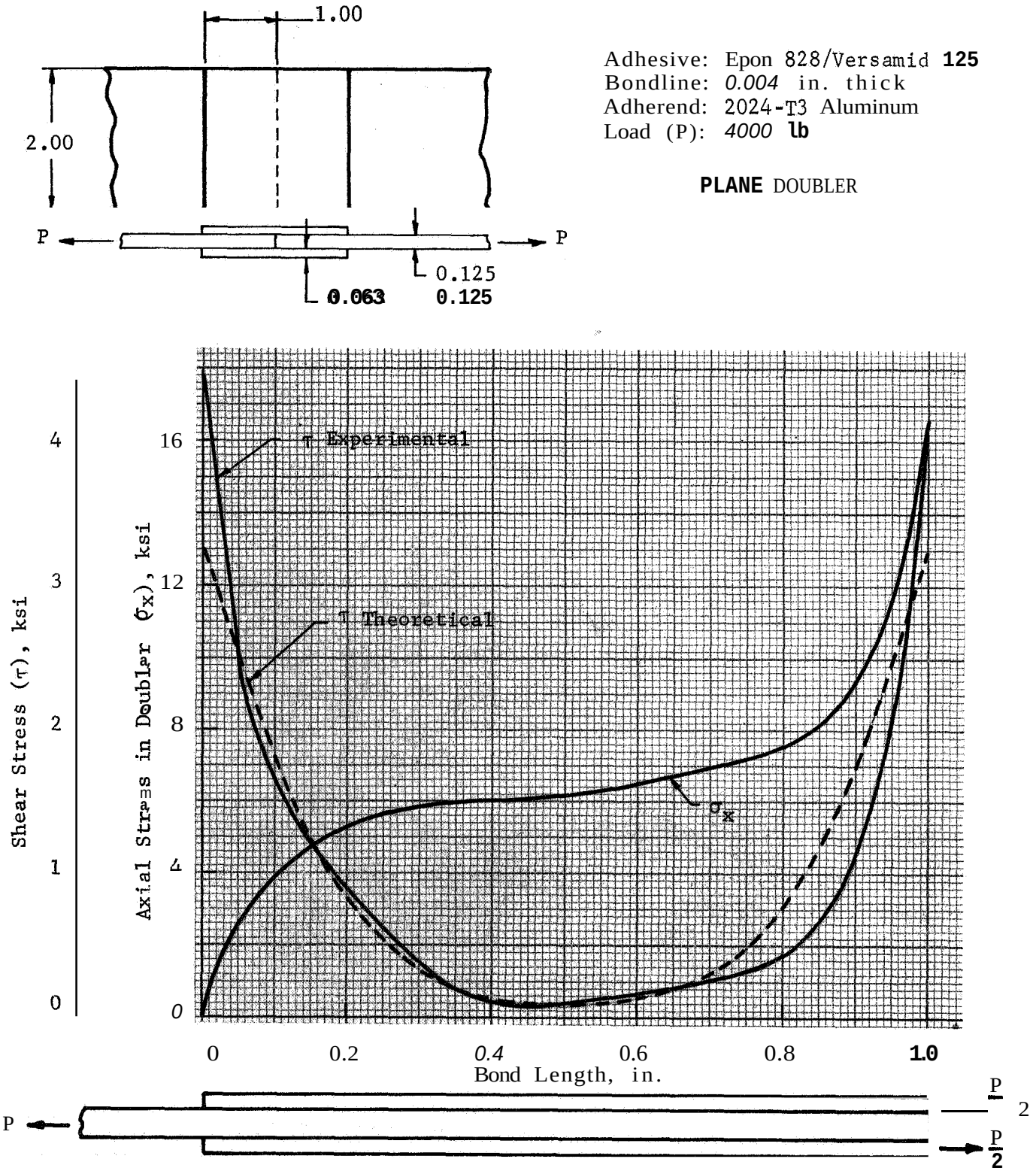

Figure 11. Stress Distribution in a Double Lap Bonded Joint (Determined by photo-stress measurement technique)

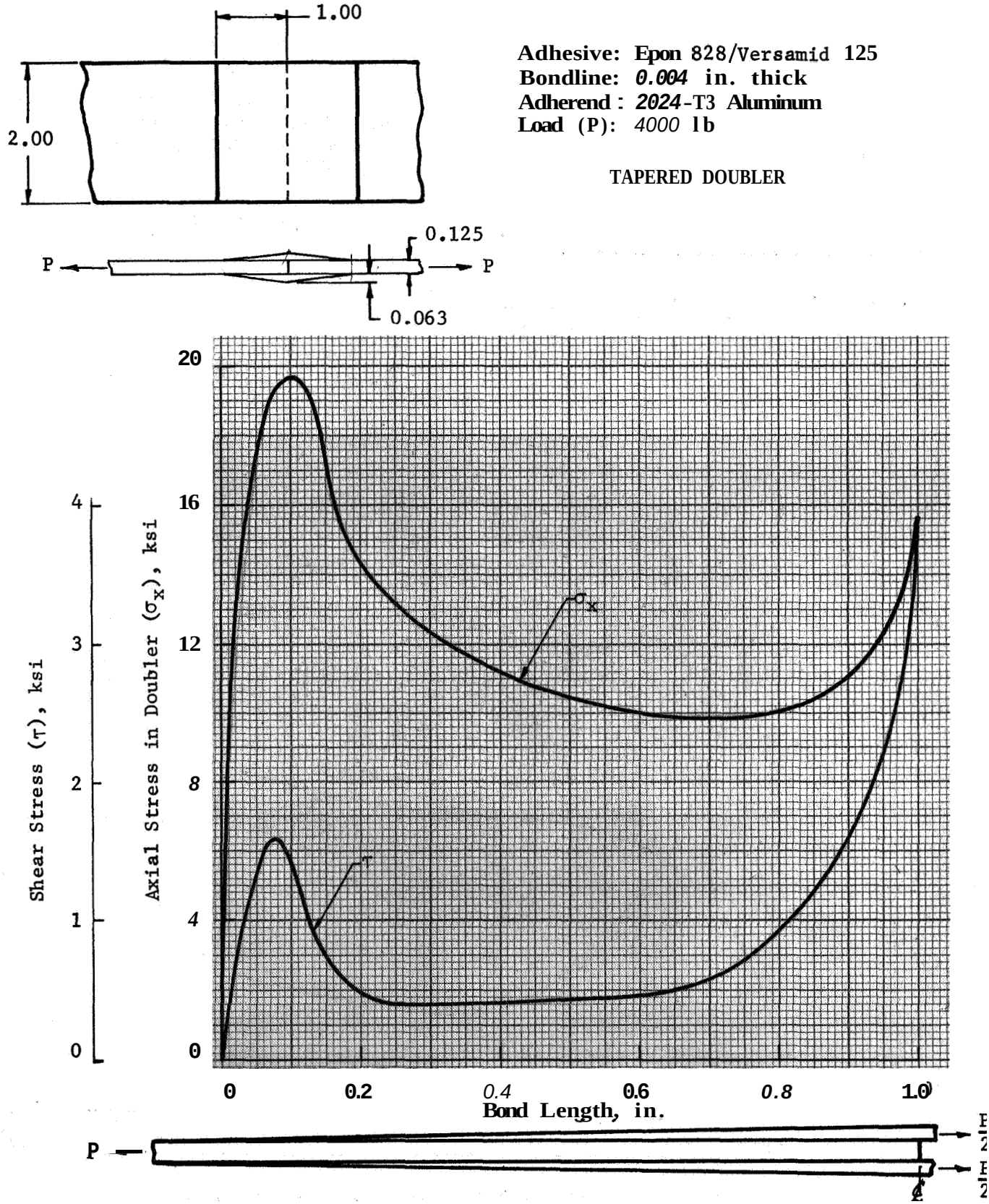

Figure 12. Stress Distribution in a Double Lap Bonded Joint (Determined by photo-stress measurement technique)

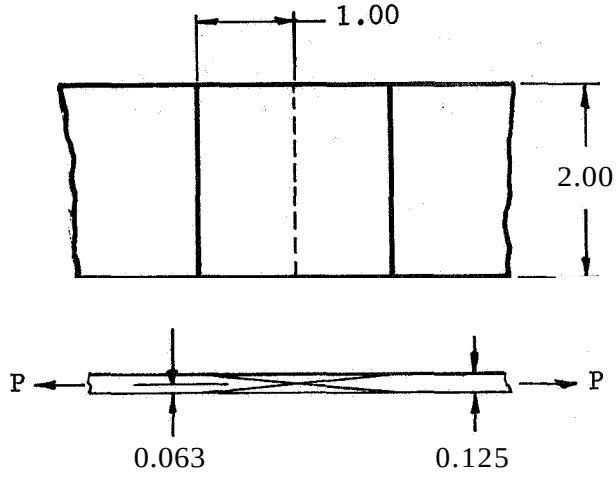

Adhesive: Epon 828/Versamid 125
Bondline : 0.004 in. thick
Adherend: 2024-T3 Aluminum
Load (P): *4000* lb

TAPERED DOUBLER **WITH** SCARFED **ADHEREND**

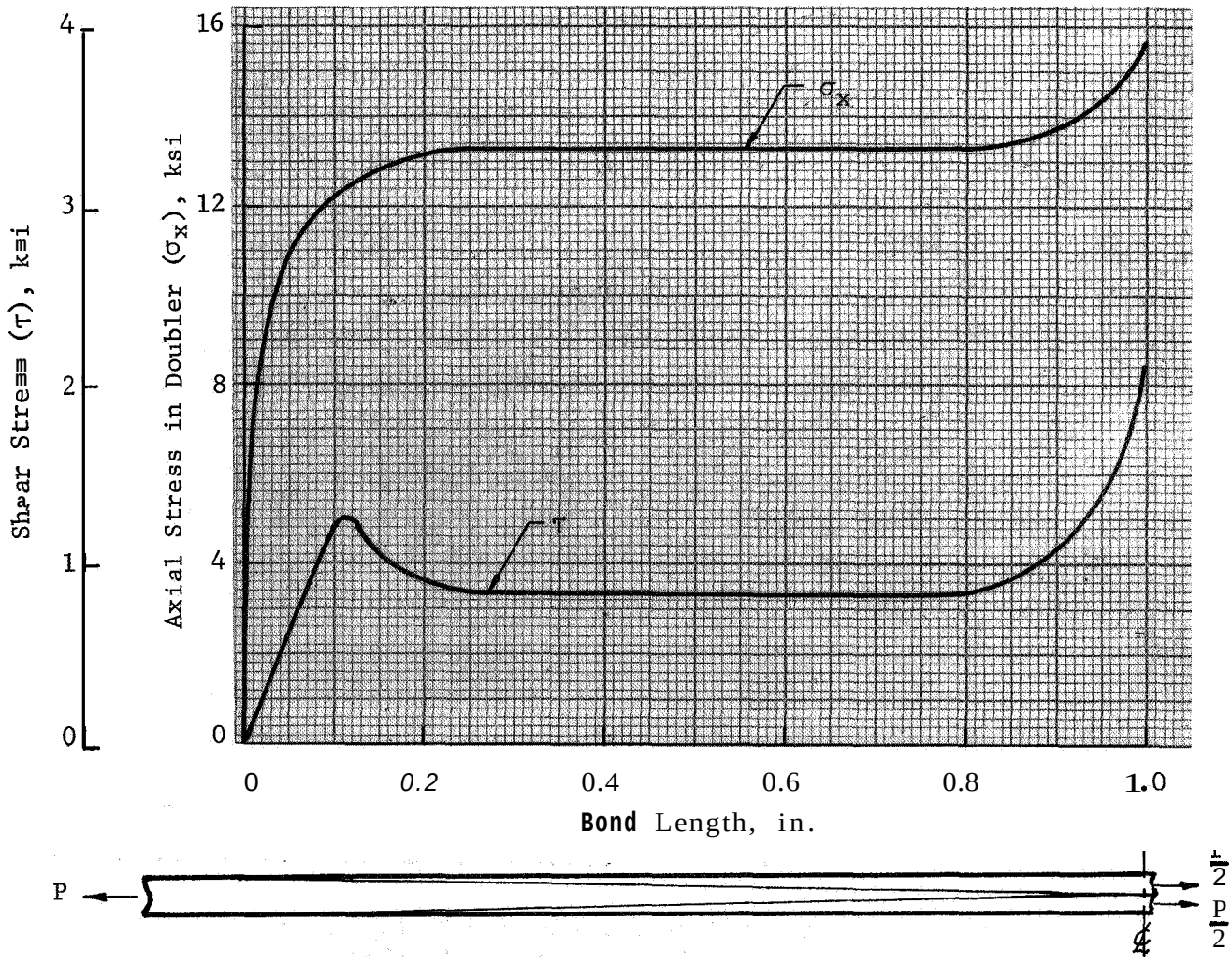

Figure **13.** Stress Distribution in a Double Lap Bonded Joint (Determined by photo-stress measurement technique)

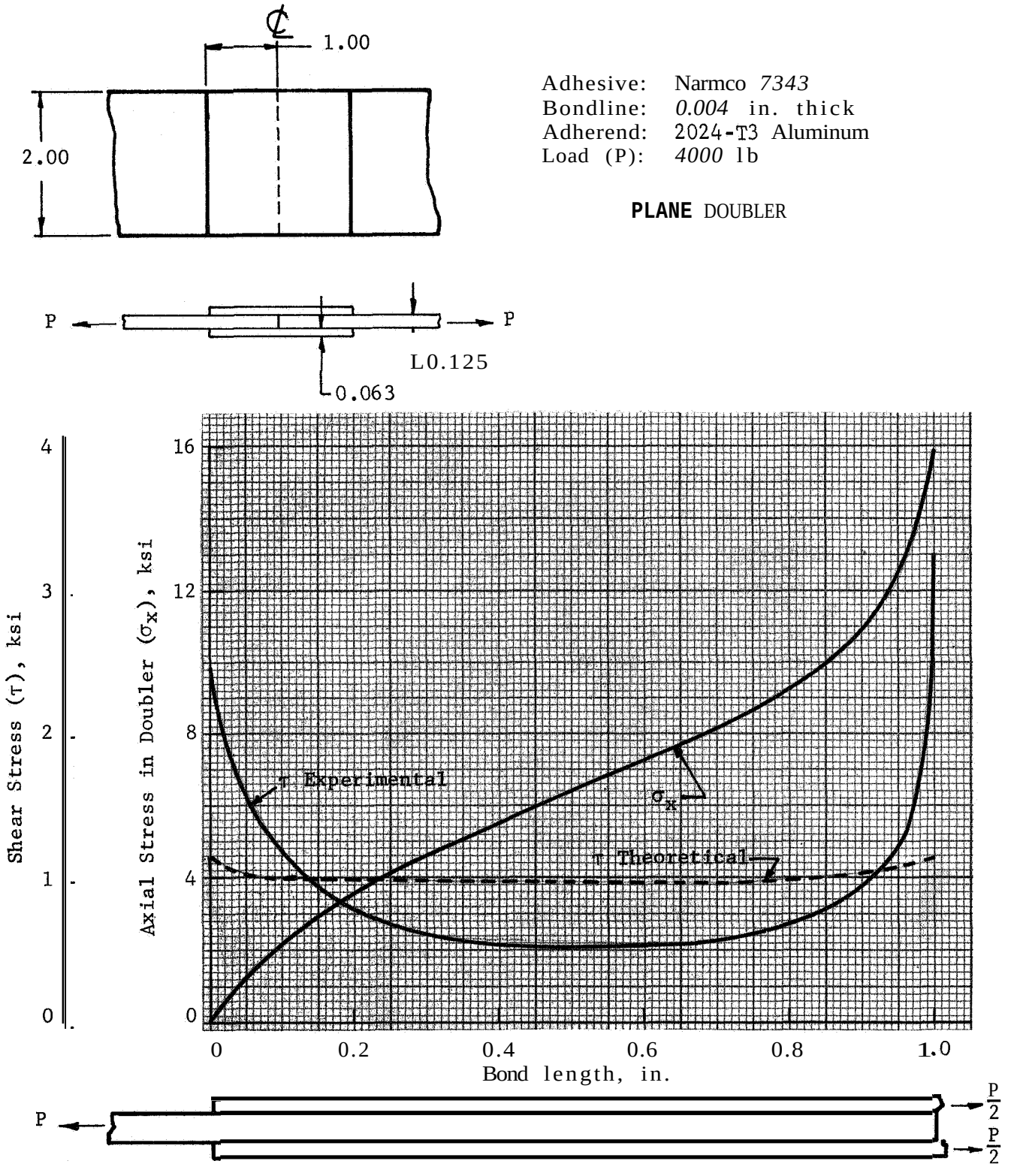

Figure 14. Stress Distribution in a Double Lap Bonded Joint (Determined by photo-stress measurement technique)

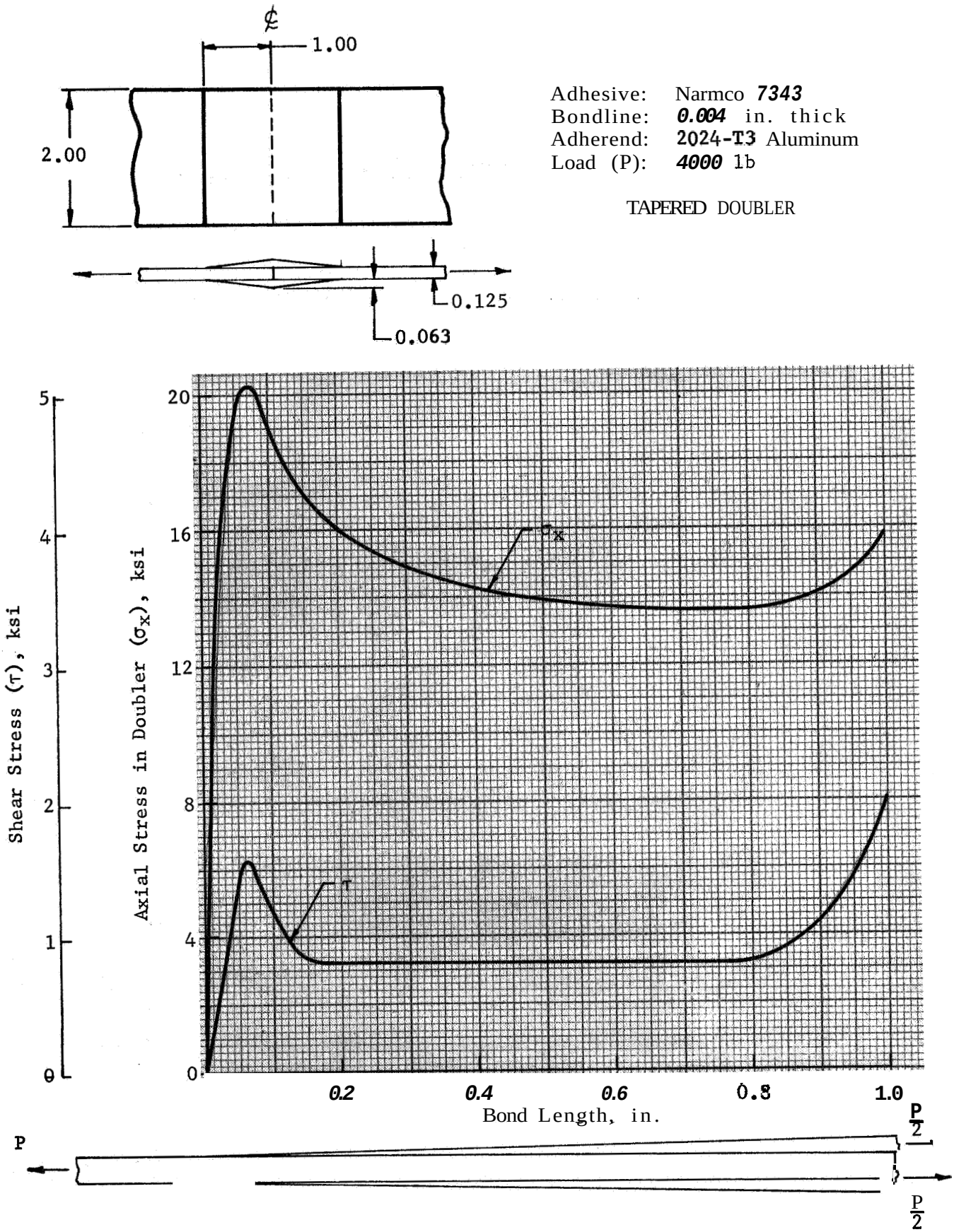

Figure 15. Stress Distribution in a Double Lap Bonded Joint (Determined by Photo-stress Measurement Technique)

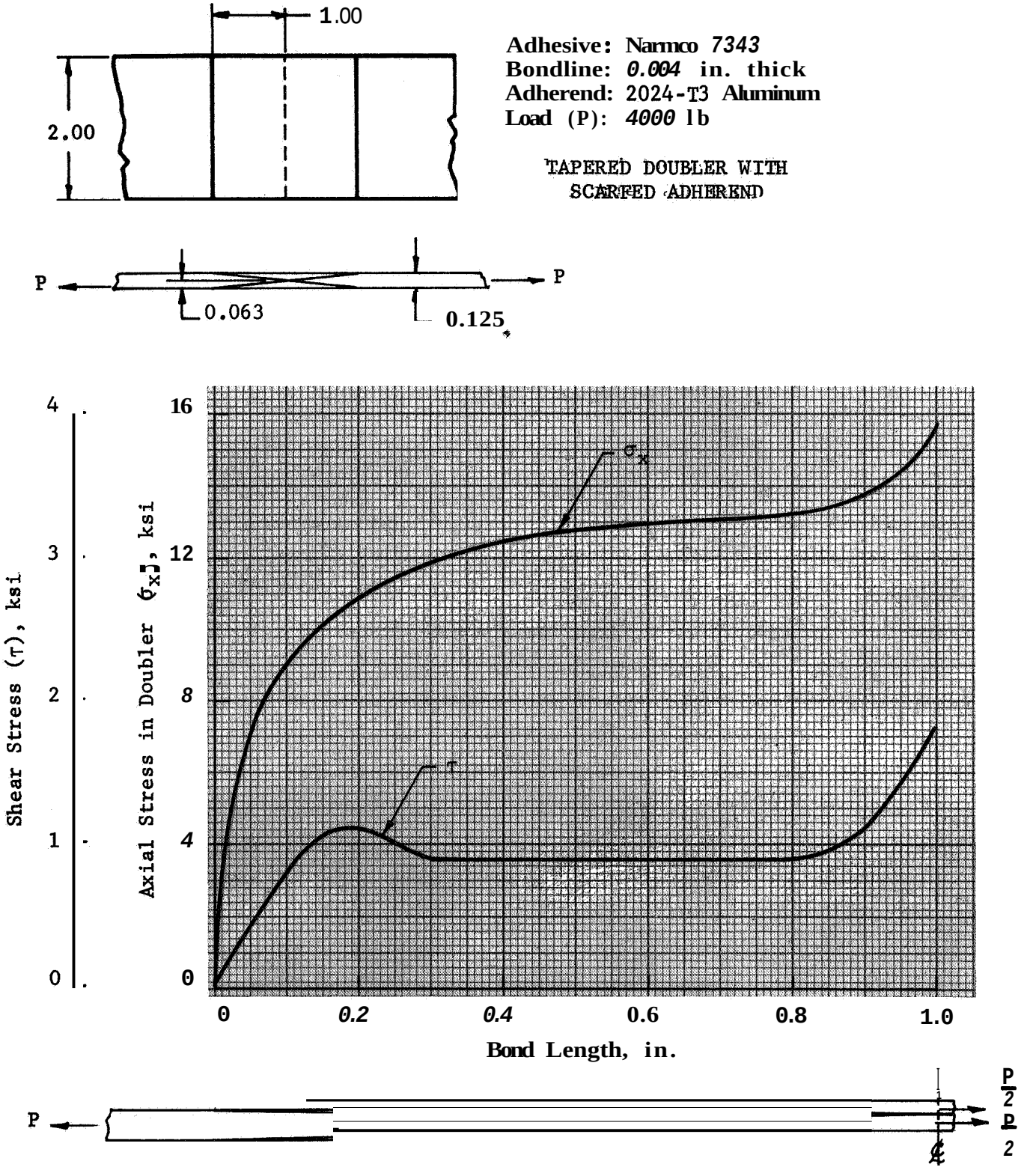

Figure 16. Stress Distribution in a Double Lap Bonded Joint (Determined by photo-stress measurement technique)

Theoretical Shear Stress Analysis

Theoretical analysis of the shear stress distribution in the plane doubler joint configuration was performed for both the epoxy and the Narmco *7343* adhesive systems. The analytical treatment of the problem follows the technique developed by Goland and Reissner[1] for single lap joints without bending. This classical analytical technique was modified so that the elastic-plastic behavior of the adhesive layer could be treated. The actual stress versus strain relationship for the adhesive is introduced in the analysis by the following approximate relationship:

$$\tau = a\left(1 - e^{-b\gamma}\right)$$

where the constants a and b are determined from experimental data. The detailed analysis is given in Appendix C.

Typical experimental shear stress versus strain data obtained during the program are presented in Figure *17* for three different adhesive systems. As pointed out previously, the curves for the Narmco *7343* system are believed to be lower than those which would represent a properly processed bond,

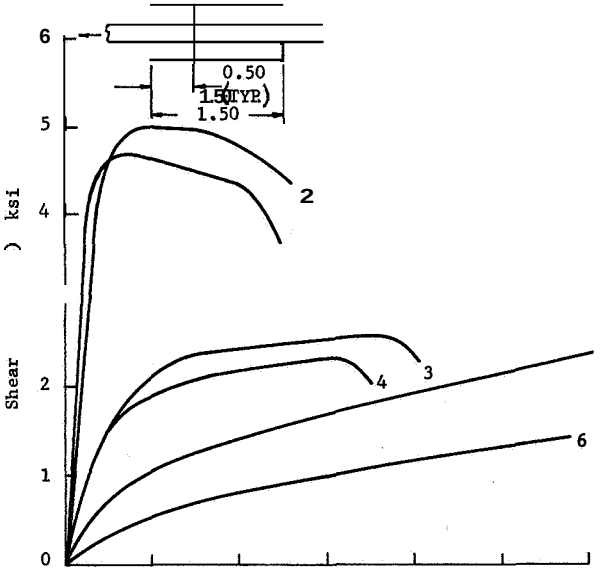

LEGEND:
1. Epon 828/Versamid 125 t_a = *0.0040*
2. Epon 828/Versamid 125 t_a = 0.0095
3. Metlbond *400* t_a = *0.0040*
4. Metlbond *400* t_a = 0.0085
5. Narmco 7343 t_a = *0.0040*
6. Nannco 7343 t_a = *0.0085*

Figure *17.* Shear Stress versus Shear Strain for Various Adhesives

The use of the exponential expression, which is best suited for approximating typical experimental stress-strain curves, complicates the mathematical problem-requiring an iterative numerical solution,

The results of the theoretical analysis of the two plane doubler joint models were shown previously in Figures 11 and 14.

SECTION III

DISCUSSION

The results of this program demonstrated that photoelastic stress analysis techniques can be used effectively to determine the shear stress distribution in the adhesive layer of bonded joints. The experimental stress analysis of bonded joints is a useful tool for the optimization of bonded joints in that it permits evaluation of the stress distribution in complex joint configurations; such an evaluation would be extremely difficult in theoretical analysis.

Only a small number of joints were investigated during this program. The limited amount of data nevertheless shows definite trends toward achieving more efficient bonded joints through improved design and manufacturing techniques.

EFFECT OF JOINT CONFIGURATION AND ADHESIVE MODULUS ON THE SHEAR STRESS DISTRIBUTION

Based on the results of the experimental stress analysis of the three different joint configurations with a high- and low-modulus adhesive, we can conclude that the shear concentration characteristics of simple bonded lap joints can be reduced by proper choices of adherends geometry and adhesive properties.

The shear stress distributions in the joints with tapered doublers show a significant reduction of the maximum stress concentrations in comparison to the plane doubler joints. The tapered scarfed joint configuration indicates even further reduction of stress concentration in the adhesive layer of both high- and low-modulus adhesives. The comparison between the results obtained for the two adhesives suggests that the lower modulus adhesive will minimize the shear stress concentrations in any joint configuration.

OPTIMUM BONDED JOINTS

The limited amount of data obtained during this program is not sufficient to establish specific design configurations for a so-called optimum bonded joint. The general trends discussed previously, however, suggest some general guidelines for the designer who is seeking more efficient bonded joints.

The experimental stress analysis data of this program are limited to symmetrical lap joints without bending. Thus, the application of these results must also be restricted to joint configurations which are not subject to bending. However, this does not necessarily mean that symmetrical configuration is required. For example, in the case of sandwich structures, a single doubler strip is commonly used for joining adjacent panels. In this case, the joint is not symmetrical but the adherends are restrained against rotation by the sandwich core; thus, the bending effects are negligible,

In an actual design analysis, we must consider practical factors in establishing a joint configuration. Tapered or contoured doubler configurations are expensive but justifiable for high-efficiency structural applications if they offer significant improvement in joint efficiency. In most applications,

the use of tapered or scarfed main plates (sandwich facings) would be prohibitive because of the associated high cost.

With these considerations in mind, then, the general joint configuration depicted in Figure 18 is a suggested high-efficiency design based on the conclusions reached during this program.

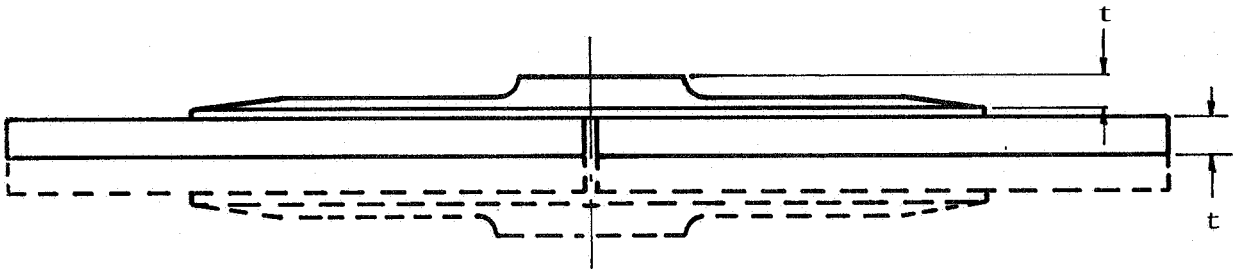

Figure 18. General Design Concept for High-Efficiency Bonded Joints

The design optimization of a given joint would be accomplished by the following procedure:

1. Adhesive material is selected based on the critical environmental requirements, such as cryogenic or high-temperature operation, high humidity or corrosive atmosphere, etc.
2. Optimum theoretical doubler configuration is calculated by numerical solution of the differential equations describing the relationship between a uniform shear stress distribution and corresponding doubler geometry. This computation technique would be based on actual shear stress-strain data for the selected adhesive, similar to the theoretical analysis performed during this program.
3. The theoretical doubler geometry resulting from the design analysis would be approximated by a practical configuration similar to the concept shown in Figure 18.

SECTION IV

RECOMMENDATIONS FOR FURTHER STUDIES

The experimental stress analysis of bonded joints resulted in a successful determination of the shear stress distribution in the adhesive layer of various configuration joints.

Our findings appear to indicate that the experimental shear stress distribution data can be combined with theoretical stress analysis techniques to provide improved design methods for efficient bonded joints, The primary limitation of existing theoretical joint analysis techniques is the elastic treatment of both the adhesives and the adherends. In actual joints, most adhesives behave plastically over a large range of the loading cycle. Therefore, the improved design methods must include elastic-plastic treatment of the adhesive and adherends.

The development of improved joint design methods requires further experimental stress analysis effort to determine the effect of overlap length, adherend configuration, adhesive thickness, and adhesive modulus on the shear stress distribution.

In addition to the experimental stress analysis work, full characterization of the mechanical proerties of the adhesives used is required. Knowledge of mechanical properties is necessary in order to obtain correlation between experimental stress distribution results and theoretical predictions, No reliable mechanical data are available, for the adhesives of interest, in the form which is directly applicable to theoretical analysis of shear stress distribution.

A special test technique was used during the current program to obtain shear stress-strain curves for adhesives under lap shear loading. This work should be extended to include testing at cryogenic temperatures and to establish creep characteristics of the adhesives.

APPENDIX A

EXPERIMENTAL STRESS ANALYSIS EQUIPMENT

The photostress analyzer equipment shown in Figure 19 was used extensively in determining the joint stress distributions. Birefringent adhesives or special plastic coatings were used in the joints under study to permit direct measurement of the mechanical strain during loading. The reflection polariscope consists of a white light source, calibrated polarizing filters, and a camera attachment for photographing the birefringent patterns.

Birefringence was measured by using the reflective polariscope and then was converted to stress distribution in the joint.

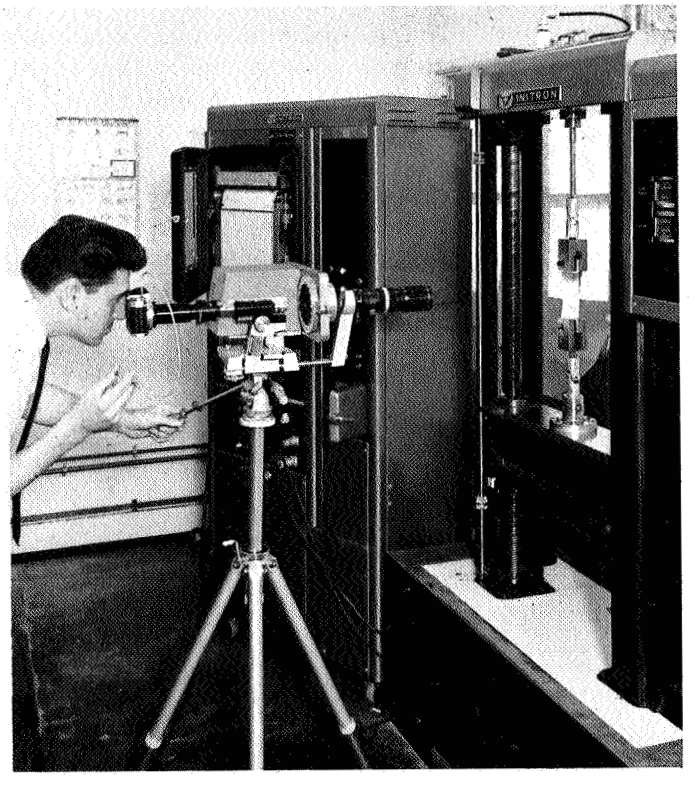

Figure 19. Photostress, Experimental Stress Analysis Equipment

APPENDIX B

CRYOSTAT FOR CRYOGENIC PHOTOSTRESS MEASUREMENTS

A special cryostat was fabricated so that photoelastic measurements could be made at cryogenic temperatures. The cryostat design is shown in Figure 20. The cryostat incorporates a large glass Dewar, which permits visual observation to be made of the submerged test specimen. The cryostat can be assembled in a test machine and the test specimen can be loaded mechanically through a self-reacting frame without introducing any loads in the glass Dewar. The cryostat is sealed at the junction with the glass Dewar and the vent line is directed upward and away from the cryostat to minimize frosting of the outer surface of the Dewar during test.

Figure 21 shows the test setup for checkout of the optical properties of the cryostat. No optical distortions could be detected in the photographs of the photoelastic fringe patterns taken in and out of the double-walled glass Dewar at room temperature.

Figures 22 and 23 show the same test specimen in the empty Dewar and submerged in liquid nitrogen. The glass bonded to the specimen was cracked as a result of thermal shock, but the photograph illustrates the excellent clarity of the specimen and shows no optical distortion in the liquid nitrogen filled cryostat.

The boiling of the liquid nitrogen was reduced to a slight bubbling within a few minutes after the cryostat was filled. Even this minimal boiling could be eliminated for short durations by closing the vent line and thereby introducing a slight pressure rise in the cryostat. Under these conditions, we were able to analyze and photograph the submerged specimen with excellent clarity.

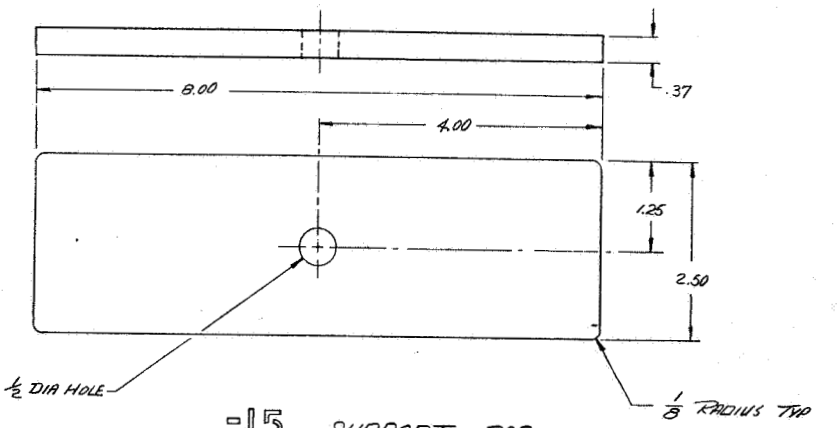

-15 SUPPORT PAD

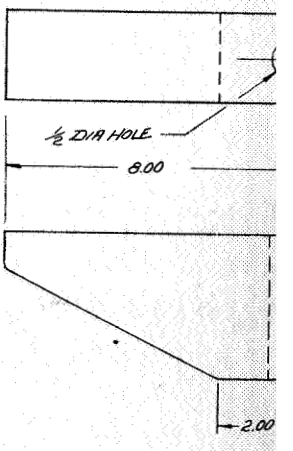

-17

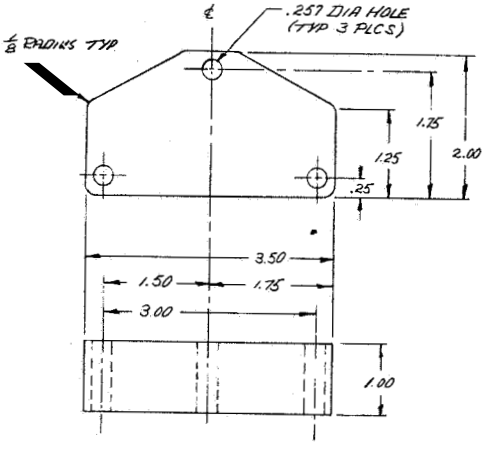

-9 SPACER

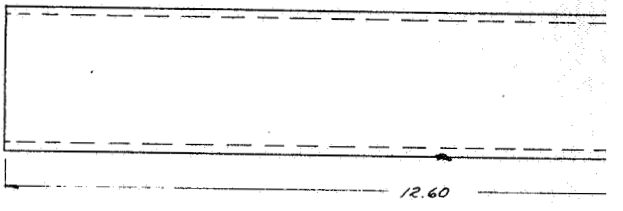

-13 TUBE

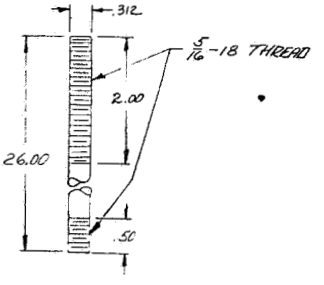

-29 ROD

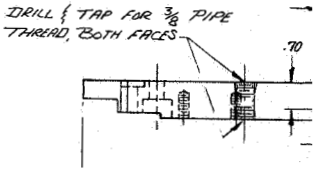

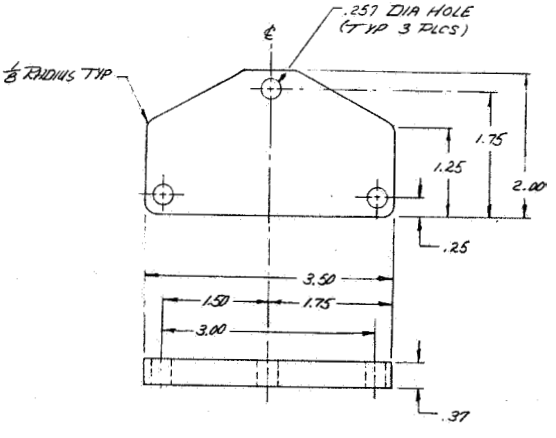

- 10 PAD

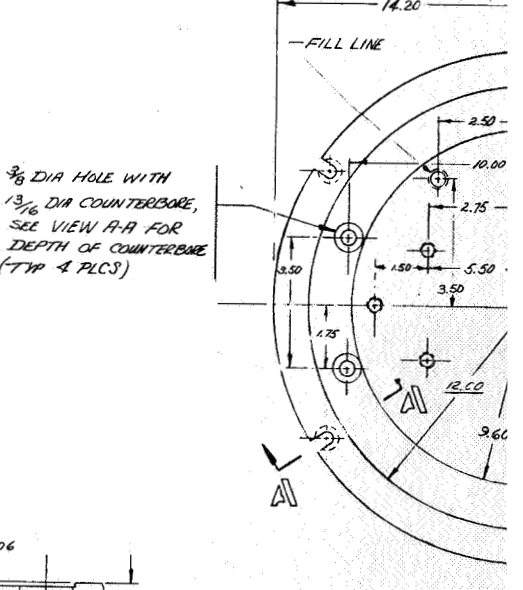

-7 B

SCALE

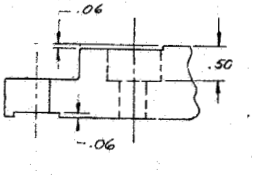

VIEW A-A

29-1

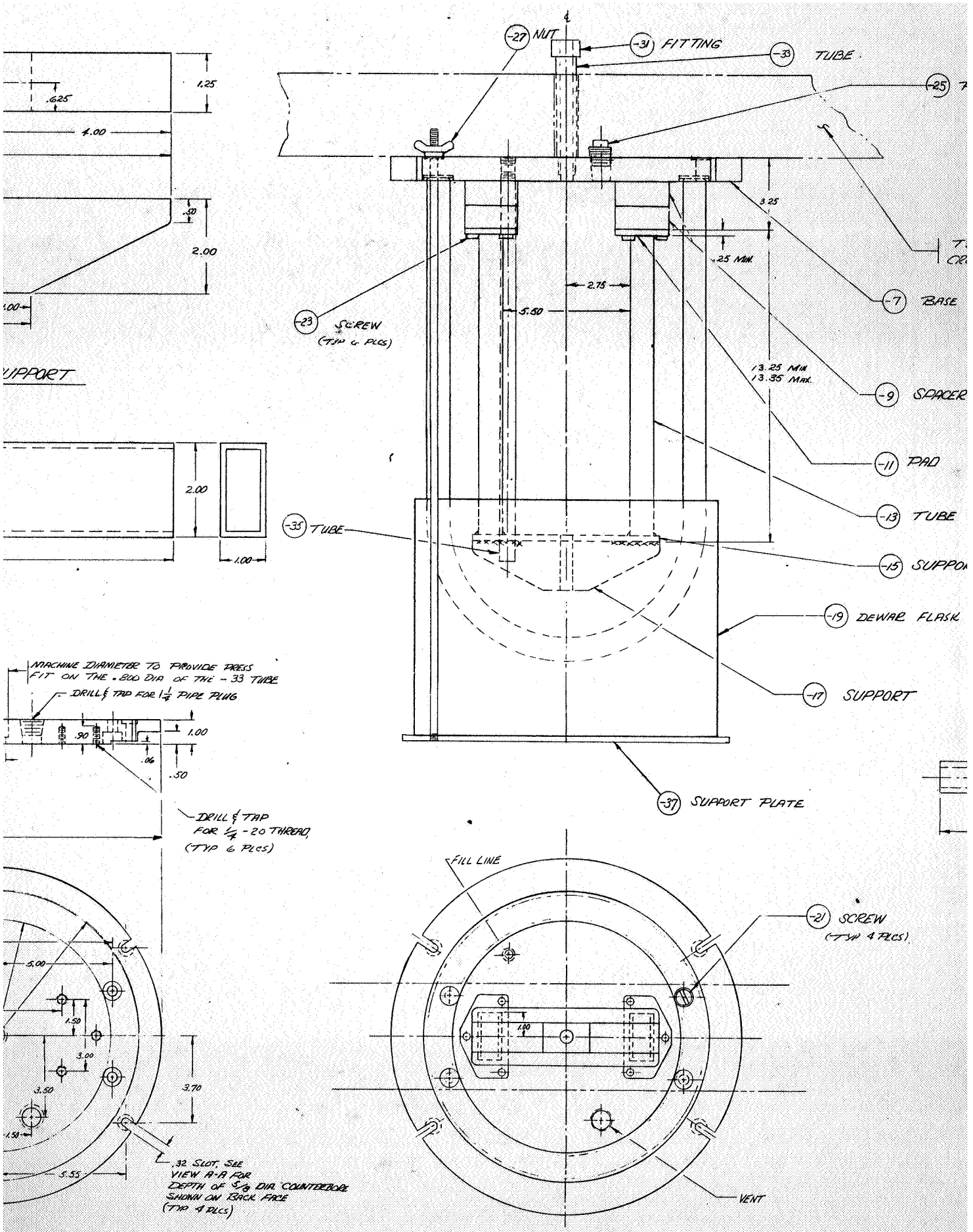

-1 CRYOSTAT ASSY

SCALE 1:2

29 - 2

NG

T MACHINE
S - HEAD

- PAD

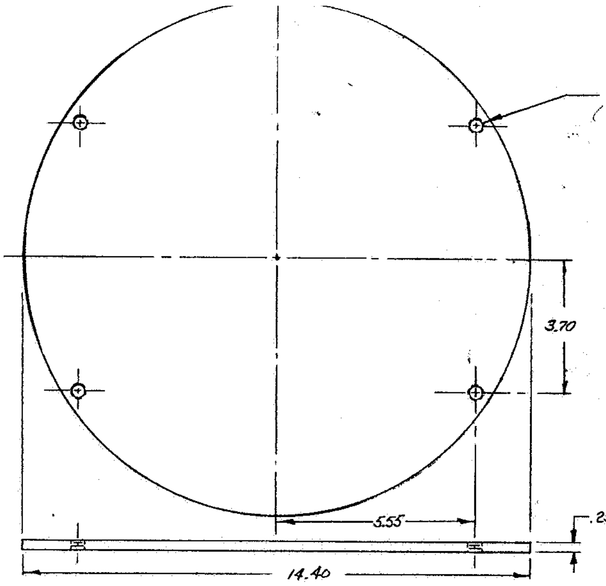

-37 SUPPORT PLATE

7. PRESS FIT & BOND (EPOXY ADHESIVE) - 33 TUBE & -7 BASE
6. SILVER SOLDER -31 FITTING TO -33 TUBE AFTER ASSEMBLY OF -31 & -33
5. HOLE THRU -7 BASE & -17 SUPPORT MUST BE PARALLEL & CONCENTRIC TO CENTERLINE OF STRUCTURE FOLLOWING FINAL ASSEMBLY
4. MACHINE -11, -13, -15, & -17 WELDMENT AS NECESSARY TO PROVIDE NORMAL, FLAT, AND PARALLEL MOUNTING SURFACES
3. JOIN -17 TO -15 BY HELI-ARC — WELD APPROX 2 INCHES IN AS SHOWN ON -1 ASSY
2. JOIN -11 & -15 TO -13 TUBE BY HELI-ARC — WELD ALONG ENTIRE CONTACT AREAS
1. -19 DEWAR FLASK MAY BE PURCHASED FROM CAL-GLASS FOR RESEARCH, INC. 3012 ENTERPRISE STREET COSTA MESA, CALIF, 92626

NOTES:

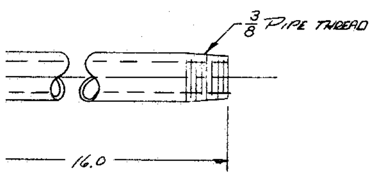

-35 TUBE

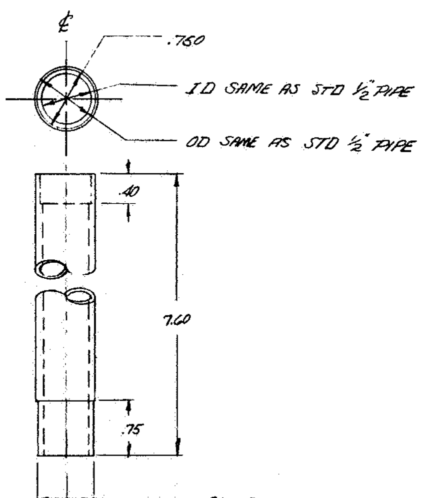

-33 TUBE

Requirements Per Assembly	Dwg. No.	Opp Dash No.	Shn Dash No.	Part Name	
1			-37	SUPPORT PLATE	1/4" × 15" DIA AL ALLOY
1			-35	TUBE	STD 3/8 BRASS PIPE 16" LONG
1			-33	TUBE	STD 1/2" BRASS PIPE 7 3/4" LONG
1			-31	FITTING	VEECO FITTING, C-50, BRASS, 1/2 ID
4			-29	ROD	5/16 DIA × 26.00, S.S
4			-27	NUT	WING NUT, 5/16-18, S.S
1			-25	PLUG	STD BRASS PIPE PLUG, 1 1/4 INCH
6			-23	SCREW	SOCKET HEAD, 1/4-20 × 3 S.S.
4			-21	SCREW	PAN HEAD, 3/8-16 × 1 1/4
1			-19	DEWAR FLASK	LG-7645 (UNSILVERED) 250 MM O.D., 500 MM DEPTH
1			-17	SUPPORT	1.25 × 2.0 × 8.0 AL ALLOY
1			-15	SUPPORT PAD	.375 × 2.5 × 8.0 AL ALLOY
2			-13	TUBE	1 × 2 × 1/8 WALL AL ALLOY
2			-11	PAD	.375 × 2 × 3.5 AL ALLOY
4			-9	SPACER	1 × 2 × 3.5 MICARTA (GLASS REINFORCED)
1			-7	BASE	1.00 t × 15 DIA MICARTA (GLASS REINFORCED)

MANUFACTURING TOLERANCES ARE UNLESS OTHERWISE NOTED:
FRACTIONS ± .031
DECIMALS .XX ± .020
.XXX ± .005
ANGLES ± 1/2 DEG
√ ALL MACHINED SURFACES & AS NOTED REF RAS 30

HEAT TREAT
FINISH

THIS DWG DASH NO | NEXT ASSEMBLY | NO. REQD

TITLE Figure 20. CRYOSTAT—PHOTO-STRESS SPECIMEN

SCALE FULL & NOTED | W.O. 399-001
DWG NO. VR-325
DWG SIZE | SHEET 1 OF 1 | CHANGE LETTER

29-3

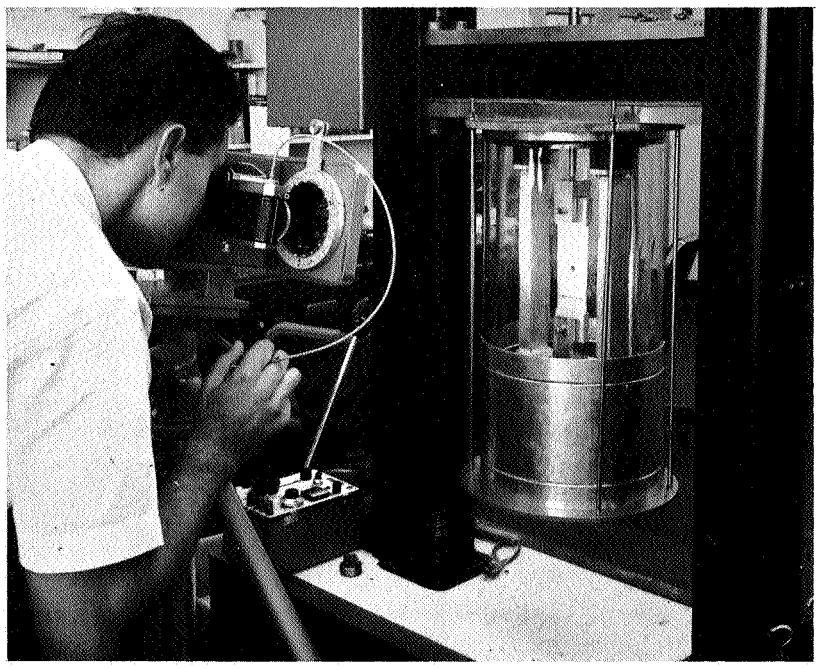

Figure 21. Optical Distortion Checkout of Dry Cryostat

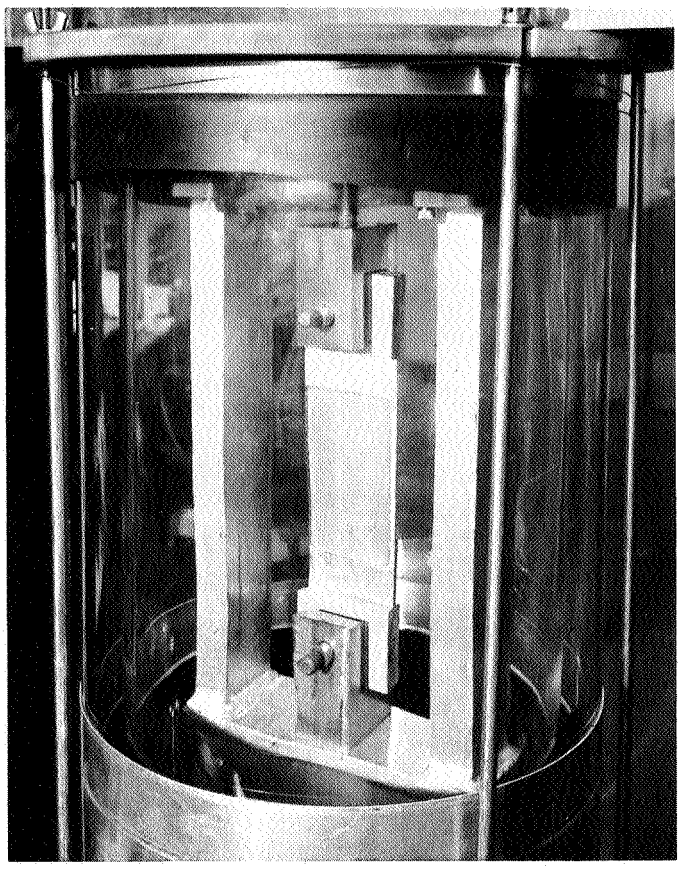

Figure 22. Close-up of Test Specimen in Dry Cryostat

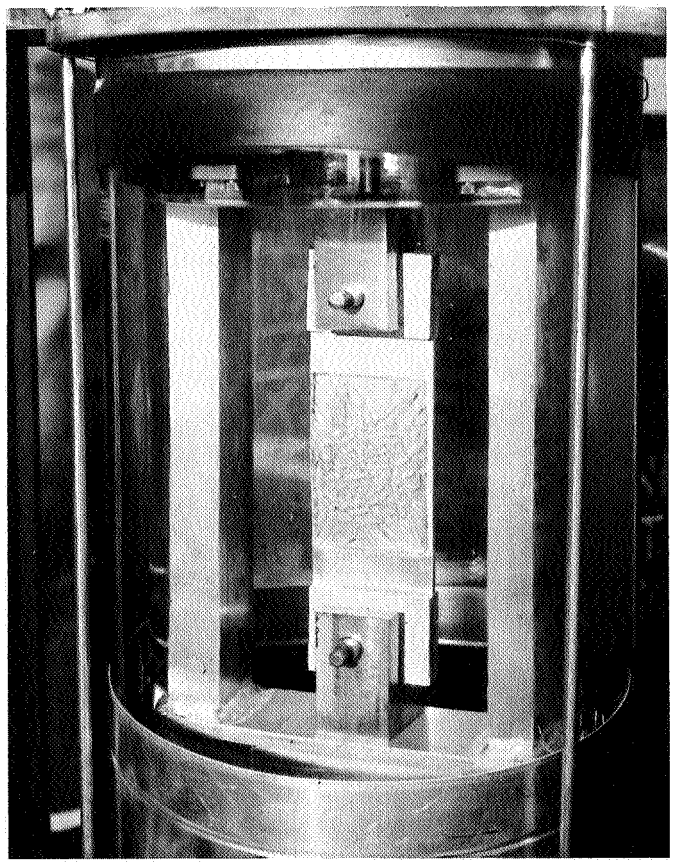

Figure 23. Close-up of Test Specimen in the Liquid Nitrogen Filled Cryostat

APPENDIX C

THEORETICAL SHEAR STRESS DISTRIBUTION IN A DOUBLE LAP BONDED JOINT

The following analysis was made on the basis of the techniques developed by Goland and Reissner.[1] The relationship between shear stress and strain in the adhesive can be written as

$$\frac{\tau}{G_c} = \gamma = \frac{u_u - u_l}{\eta}$$

where u_u and u_l are the displacements of the two adherends. Differentiating with respect to x,

$$\frac{d\gamma}{dx} = \frac{1}{\eta}\left(\frac{du_u}{dx} - \frac{du_l}{dx}\right)$$

The adherend stress-strain relationships give

$$\left.\begin{aligned} \frac{du_u}{dx} &= \frac{1}{E}\left(\frac{T_u}{t} - 6\frac{M_u}{t^2}\right) \\ \frac{du_l}{dx} &= \frac{1}{E}\left(\frac{T_l}{t} + 6\frac{M_l}{t^2}\right) \end{aligned}\right\}$$

For the double lap joint configuration being considered, the moments are zero. Typical joint configurations used are depicted in Figure 24.

$$\frac{d\gamma}{dx} = \frac{1}{Et\eta}\left(T_u - T_l\right)$$

Differentiating once more,

$$\frac{d^2\gamma}{dx^2} = \frac{1}{Et\eta}\left(\frac{dT_u}{dx} - \frac{dT_l}{dx}\right)$$

$$= \frac{1}{Et\eta}\left(\tau_o + \tau_o\right) = \frac{2\tau_o}{Et\eta}$$

Assuming a relationship between shear stress and shear strain of the form

$$\tau = a\left(1 - e^{-b\gamma}\right)$$

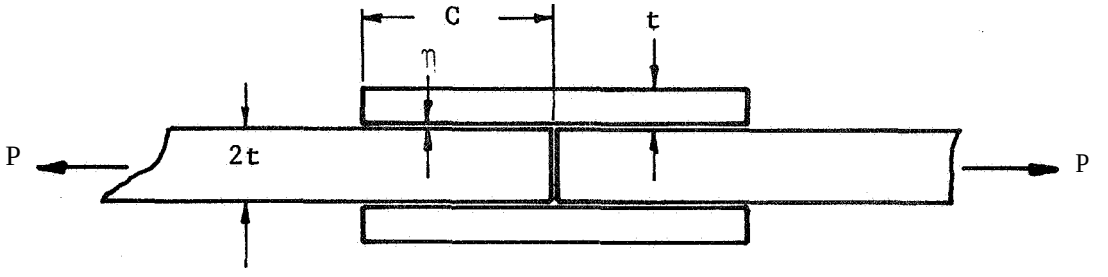

Test Specimen

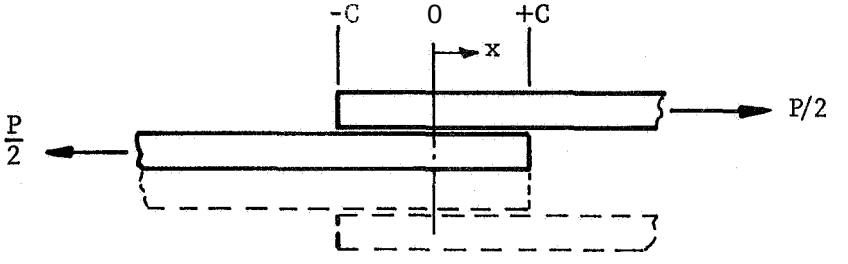

Analytical Model

$\frac{P}{2} = ptw$

$w = 2.00$

$t = 0.063$

$C = 0.50$

$\eta = 0.004$

$E = 107$

Figure 24. Typical Joint Configuration Used in Theoretical Analysis

for the adhesive, we have

$$\frac{d^2\gamma}{dx^2} = \frac{2a}{Et\eta}\left(1 - e^{-b\gamma}\right)$$

Now, let $y = \frac{d\gamma}{dx}$.

$$\frac{d^2\gamma}{dx2} = y\,\frac{dy}{d\gamma}$$

$$ydy = \frac{2a}{Et\eta}\left(1 - e^{-b\gamma}\right) d\gamma$$

Integrating both sides,

$$\frac{y^2}{2} = \frac{2a\gamma}{Etq} + \frac{2a}{Etq}\,\frac{1}{b}\,e^{-b\gamma} + c_1$$

or

$$\left(\frac{d\gamma}{dx}\right)^2 = \frac{4}{Et\eta}\,\frac{a}{b}\,e^{-b\gamma} + \frac{4}{Et\eta}\,a\gamma + c_2$$

Applying boundary conditions, at $x = -c$, $\gamma = \gamma_{max}$

$$\frac{d\gamma}{dx} = \frac{T}{Et\eta} = \frac{pt}{Et\eta}$$

$$\left(\frac{pt}{Et\eta}\right)^2 - \frac{4}{Et\eta}\,\frac{a}{b}\,e^{-b\gamma_{max}} - \frac{4}{Et\eta}\,a\gamma_{max} = c_1$$

and

$$\left(\frac{d\gamma}{dx}\right)^2 = \left(\frac{4}{Et\eta}\,\frac{a}{b}\,e^{-b\gamma} + a\gamma\right) + \left(\frac{pt}{Et\eta}\right)^2 - \frac{4}{Et\eta}\left(\frac{a}{b}\,e^{-b\gamma_{max}} + a\gamma_{max}\right)$$

Nondimensionalizing,

$$\left[\frac{d\gamma}{d\left(\frac{x}{c}\right)}\right]^2 = \frac{4c^2}{Et\eta}\left(\frac{a}{b}\,e^{-b\gamma} + a\gamma\right) + \left(\frac{ptc}{Et\eta}\right)^2 - \frac{4c^2}{Et\eta}\left(\frac{a}{b}\,e^{-b\gamma_{max}} + a\gamma_{max}\right)$$

$$\left[\frac{d\gamma}{d\left(\frac{x}{c}\right)}\right]^2 = \frac{4}{b}\frac{G_c}{E}\frac{c}{t}\frac{c}{\eta}\left(\frac{e^{-b\gamma}}{b}+\gamma\right)+\left(\frac{p}{E}\frac{c}{\eta}\right)^2-\frac{4}{b}\frac{G_c}{E}\frac{c}{t}\frac{c}{\eta}\left(\frac{e^{-b\gamma_{max}}}{b}+\gamma_{max}\right)$$

$$\frac{d\gamma}{d\left(\frac{x}{c}\right)} = \left[\alpha_1\left(\frac{e^{-b\gamma}}{b}+\gamma\right)+\alpha_2\right]^{\frac{1}{2}}$$

where

$$\alpha_1 = \frac{4}{b}\frac{G_c}{E}\frac{c}{t}\frac{c}{\eta}$$

$$\alpha_2 = \left(\frac{p}{E}\frac{c}{\eta}\right)^2-\alpha_1\left(\frac{e^{-b\gamma_{max}}}{b}+\gamma_{max}\right)$$

No general solution could be found for an equation of this form. An iterative solution was therefore required. At

$$\frac{x}{c} = -1 \quad , \quad \gamma = \gamma_{ult}$$

Once the value of y and $d\left(\frac{x}{c}\right)$ is known for any value of $\frac{x}{c}$, the value of y at $\frac{x}{c}+\Delta\frac{x}{c}$ is found from

$$\gamma\Big|_{\frac{x}{c}+\Delta\frac{x}{c}} = \gamma\Big|_{\frac{x}{c}} + \left.\frac{d\gamma}{d\left(\frac{x}{c}\right)}\right|_{\frac{x}{c}}\Delta\frac{x}{c}$$

The value of $d\left(\frac{x}{c}\right)$ at $\frac{x}{c}+\Delta\frac{x}{c}$ is found by substituting y at $\frac{x}{c}+\Delta\frac{x}{c}$ into equation (1). The operation is then repeated for

$$\gamma\Big|_{\frac{x}{c}+2\Delta\frac{x}{c}} = \gamma\Big|_{\frac{x}{c}} + \left.\frac{d\gamma}{d\frac{x}{c}}\right|_{\frac{x}{c}}\Delta\frac{x}{c}$$

The process is repeated throughout the range of $\frac{x}{c}$ required. The smaller the value for $\Delta \frac{x}{c}$ used in the analysis, the more accurate will be the results.

The iteration technique yields a value of $\frac{\tau}{p}$ for each value of $\frac{x}{c}$ from the joint parameters

$$\frac{c}{t} \ , \ \frac{c}{\eta} \ , \ \frac{p}{E} \ , \ \frac{G_c}{E} \ , \ b \ , \text{ and } \gamma_{max}$$

The shear stress distribution in the joint can then be plotted graphically from these data.

REFERENCES

1. M. Goland and E. Reissner, "The Stresses in Cemented Joints," Journal of Applied Mechanics, March 1944

2. Forest Products Laboratory, Stresses in a Lap Joint with Elastic Adhesives, FPL Report No. 1864, Madison, Wisconsin, September 1957

3. Mechanics of Adhesive-Bonded Lap Type Joints, Technical Documentary Report No, MIL TDR-64-298, October 1964

4. 0. Volkersen, "Shear Stress Distribution in Bonded Joints," Journal Energie & Technick, May 1953